"Synthesis and Characterization of Cadmium Selenide Quantum dots Nanoparticles"

A

Project Report

Submitted in partial fulfillment of the requirement for the award

Of the degree of

MASTER OF TECHNOLOGY

In

NANOSCIENCE AND TECHNOLOGY

By

DEEPIKA SANDIL

Roll no. 03/NST/ 2K11

Under the Guidance of

Dr. N. K. Puri

Assistant Professor

DTU, New Delhi

DEPARTMENTNT OF APPLIED PHYSICS

DELHI TECHNOLOGY UNIVERSITY

NEW DELHI – 110042

JULY - 2013

Department of Applied Physics

Delhi Technological University

Delhi

CERTIFICATE

This is to certify that Mrs. Deepika Sandil, a student of final semester M. Tech. (Nanoscience and Technology), Applied Physics Department, during the session 2011-2013 has successfully completed the project work on **"Synthesis and Characterization of Cadmium Selenide Quantum Dot nanoparticles"** at DTU, Delhi **and** has submitted a satisfactory report in partial fulfillment for the award of the degree of Master of Technology.

The assistance and help received during the course of investigation have been fully acknowledged. She is a good student and we wish her good luck in future.

Dr. N. K. Puri
Assistant Professor,
Applied Physics Department
Delhi Technological University
Delhi - 110042

Prof. S.C. Sharma
HOD
Applied Physics Department
Delhi Technological University,
Delhi - 110042

Candidate Declaration

I hereby declare that the work which is being presented in this thesis entitled **"Synthesis and Characterization of Cadmium Selenide Quantum Dot nanoparticles" is my** own work carried out under the guidance of Dr. N. K. Puri, Assistant Professor, Delhi Technological University, and Delhi.

I further declare that the matter embodied in this thesis has not been submitted for the award of any other degree or diploma.

Date: Deepika Sandil

Place: New Delhi Roll No. - 2K11 /NST/03

Acknowledgements

With great pleasure I would like to express my first and sincere gratitude to my Supervisor **Dr. N. K. Puri** for his continuous support, patience, motivating ideas , enthusiasium and immense knowledge. His guidance always enlightens and helped me to shape my work.

Besides my Supervisor , I would like to express my deep gratitude and respect to Dr. **S.C. Sharma** , Prof. and Head of Department of Physics, DTU, for his encouragement , insightful comments and valuable suggestions during the course.

My sincere thanks also go **to Dr. R.K Sinha Sir, Dr. Pawan Tyagi, Dr. M. Jayasimhadri, and Dr. Mohan S. Mehata, Dr. Ajeet Kumar and Dr. Amrish K. Panwar Sir** for their valuable advices and stimulating discussions throughout my course work. Thanks them for questioning me about my ideas, helping me think rationally and even for hearing my problems.

I would also like to thanks my supportive friends and others who made specially, the labs a friendly environment for working.

Last but not the least , I would like to thanks **my family, my mother, my father, my father in-law and specially my husband** for always believing in me, for their continuous love and their supports in my decision, without whom I could not have made it here.

DEDICATED TO

MY

MOTHER IN –LAW

WITH LOVE

NAVYA SANDIL

List of Figures

Figure Name **Page no.**

ABSTRACT

Semi-conductor nanocrystals, so called Quantum dots have been of great interest for both fundamental research and technical applications due to its novel physical and optical properties. Among the various materials used for fabrication, Cadmium Selenide (CdSe) nanoparticles have drawn much attention because of its potential application and variety of methods of its preparation.

In this project we have synthesized CdSe NCs using colloidal chemistry which has used the Green Chemistry technique by considering Oleic acid and paraffin oil as the solvent in the solution and CdO and Se powder as precursors. The advantages of this method include the low–cost, environment friendly, fast and mass production of CdSe NCs with the desired quality.

The synthesized CdSe nanoparticles were characterized by powder XRD, FTIR, UV- Visible, photoluminescence and Raman spectroscopy. The Raman spectra were in good agreement with XRD peaks confirming the formation of CdSe NCs. Also FTIR studies reveal the presence of capping agent Oleic acid on the CdSe NCs.

Contents

Chapter 1

NANOTECHNOLOGY

Nanotechnology is the study of manipulating matter on an atomic and molecular scale. Generally , it deals with developing materials , devices , or other structures Possessing at least one dimension sized from 1 to 100 nanometers. And at this quantum – realm scale, quantum mechanical effects becomes important.

Nanotechnology is very diverse, ranging from extensions of conventional device physics to completely new approaches based upon molecular self – assembly. It is valuable in developing new materials with dimensions on the nanoscale to investigating whether we can directly control matter on the atomic scale. Nanotechnology evokes the application of fields of science as diverse as surface science , organic chemistry , molecular biology , semiconductor physics , micro – fabrication , etc. [3].

1.1 HISTORY

Although nanotechnology is a relatively recent development in scientific research, the development of its central concepts happened over a longer period of time. In 1974, Norio Taniguchi introduced the term "Nanotechnology" to represent extra – high precision and ultra – fine dimensions, and also predicted improvements in integrated circuits, optoelectronic devices and computer memory devices. The emergence of nanotechnology in the 1980s was caused by the convergence of experimental advances such as the invention of the scanning tunneling microscope in 1981 and the discovery of fullerenes in 1985. The scanning tunneling microscope, an instrument for imaging surfaces at the atomic level, was developed in 1981 by Gerd Binning and Heinrich Rohrer at IBM Zurich Research Laboratory, for which they received the Nobel Prize in Physics in 1986. Fullerenes were discovered in 1985 by Harry Kroto, Richard Smalley, and Robert Curl, who together won the 1996 Nobel Prize in Chemistry.

Around the same time, K. Eric Drexler developed and popularized the concept of nanotechnology and founded the field of Molecular nanotechnology. In 1979, Drexler encountered Richard Feynman's 1959 talk "There's Plenty of Room at the Bottom" [1]. The term "nanotechnology", originally coined by Norio Taniguchi in 1974, was unknowingly appropriated by the Drexler in his 1986 book "Engines of Creation: The Coming Ero Nanotechnology"[3], which proposed the idea of a nanoscale "assembler" which would be able to build a copy of itself and of other items of arbitrary complexity. Drexler's vision of nanotechnology is often called "Molecular Nanotechnology" (MNT) or "molecular manufacturing," and Drexler at one point proposed the term "zettatech" which never became popular.

In the early 2000s, the field was subject to growing public awareness and controversy, with prominent debates about both its potential implications, exemplified by the Royal Society's report on nanotechnology, as well as the feasibility of the applications envisioned by advocates of molecular nanotechnology, which culminated in the public debate between Eric Drexler and Richard Smalley in 2001 and 2003. Many nations moved to promote and fund research into nanotechnology with programs such as National Nanotechnology Initiative, Centre for Nanotechnology. The early 2000s also saw the beginnings of commercial applications of nanotechnology, although these were limited to bulk applications of nanomaterials, such as the Silver, Nano platform for using Silver Nano platform for using silver nanoparticles as an antibacterial agent, nanoparticles-based transparent sunscreens, and carbon nanotubes for stain-resistant textiles.

1.2 Basic Concepts

One nanometer (nm) is one billionth, or 10^{-9}, of a meter. By comparison, typical carbon-carbon bond lengths, or the spacing between these atoms in a molecule, are in the range 0.12-0.15 nm, and a DNA double-helix has a diameter round 2 nm. On the other hand, the smallest cellular life-forms, the bacterial of the genus Mycoplasma, are round 200 nm in length. By convention, nanotechnology is taken as the scale range I to 100 nm following the definition used by the National Nanotechnology Initiative in the US. The lower limit is set by the size of atoms since nanotechnology musty build its devices from atoms and molecules. The upper limit is more or less arbitrary but is around the size that phenomena not observed in large structures start to become apparent and can be made use of in the nano devices. These new phenomena make nanotechnology distinct from devices which are merely miniaturized version of an equivalent macroscopic device; such devices are on the great scale and come within the description of micro technology. As dimensions minimize to nanolevel the following changes come to the picture:

- Larger Surface to Volume Ratio
- Quantum Confinement
- Quantized Energy States

According to Dr. K. Eric Drexler there are some things that become practical with mature Nanotechnology [1];

- Nearly free consumer products
- PCs billions of times faster than today

- Safe and affordable space travel
- Virtual end to illness, aging, death
- No more pollution and automatic cleanup of existing pollution
- End of famine and starvation
- Reintroduction of many extinct plants and animals.

Properties of the solids are dependent on their size. The properties of the bulk materials are mostly retained till the reduction of their dimensions in micrometer range. However, as the size of materials is reduced to nanomaterials. For example, consider the case of nano gold particles , it does not show characteristic yellow color at this scale but show different colors, orange, red, purple or greenish depending upon the actual size of the particles. Compared to bulk, the melting point and chemical properties also change when the material is reduced to nanoform. The melting temperature of nano form reduces significantly. Bulk semiconductors become insulators when dimensions are reduced to nanometers. The primary cause for the drastic change in behavior of nanomaterials compared to their bulk form is that in nano form the number of atoms on the surface is a big fraction of the total number of atoms in the material i.e. large surface to volume ratio.

1.3 NANOPARTICLES: Deviation from Bulk Behavior

Nanoparticles are generally considered to be the structures, consisting of atoms or molecules, with a radius less than 100 nm (or 1000 A^0 as 1 nm = 10 A^0). As the number of atoms increases in a cluster; the percentage of atoms on the surface decreases. It is the presence of large percentage of atoms on the surface in the nanostructures, which make them behave differently compared to the bulk structures.

Also, the physics and chemistry of nanostructures are different than that of the bulk structures. Particles of different sizes scatter different wavelengths of light. This fact has been used from ancient times to produce beautiful colors in stained-glass, due to the presence of the nano metal-clusters in the glass having size comparable to the wavelength of light. What makes nanoparticles very interesting and endows them with their unique properties is that their size is smaller than critical lengths that characterize many physical phenomena. Generally, physical properties are associated with some characteristic length such as scattering length, thermal diffusion length, etc. The electrical resistance of a metal is dependent upon the mean free path or scattering length, the electrons travel between any two successive collisions.

1.4 Dimension Effects

When the size of a material is reduced to nanometer range (<100nm), there is a marked change in the properties of the material. If one dimension is reduced to the nano-range but the other two dimensions remain large, then the structure is known as a quantum well. If two dimensions are reduced to nano-range but one of the dimensions remains large, the resulting structure is quantum wire. When all the three dimensions are in nanometer range, the structure is referred to as a quantum dot.

The confinement of a particle in one dimension, two dimensions and three dimensions can be deal as the case of **"particle in a potential box"**.

For a particle in a box of length **a** with potential

v = 0 $0 < x < a$

$v = \infty$ $x < 0$ or $x > a$

The solution of the Schrodinger equation yields eigenvalues.

$$\boldsymbol{E_n = \frac{(n^2 * h^2)}{8 * m * a^2}} \qquad \textbf{...(1.1)}$$

And eigenfuctions as

$$\varphi = A \sin(\frac{n*\pi}{a})x \qquad \ldots(1.2)$$

1.5 Density of States

Density of status *D(E) is defined as the number of states per unit energy range (E and E+ dE)*. It is an important parameter as it helps in understanding various spectroscopic and transport properties of materials. As the energy of a particle in a one-dimensional box is

$$\mathrm{E_n} = \frac{h^2 n^2}{8ma^2}$$

$$\frac{dn}{dE} = \frac{8ma^2}{h^2}\frac{1}{2n} = \frac{a}{h}\frac{\sqrt{2m}}{E}$$

Or

$$D(E) \propto E^{-1/2} \quad \text{…. (1.3)}$$

This shows that the density of states varies with energy and it is inversely proportional to the square root of energy. We discuss below the variation or density of states for solids of different dimensions.

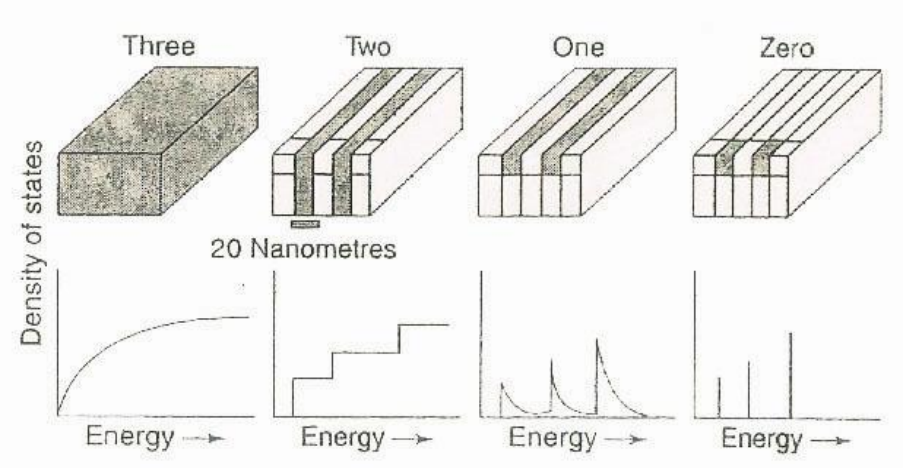

Figure - A: density of state Vs Energy (Graph)

1.5.1 Density of States for a Zero Dimensional (0D) Structure

In zero dimensional structures, like quantum dots, an electron is confined in a three-dimensional potential box with extremely small (<100 nm) length, breadth and height as a 0D solid. All three spatial directions are quantized and the expression for the density of states follow a δ-functional given as

$$D(E) = \Sigma\delta\,(E - \varepsilon_i) \quad \text{…(1.4)}$$

Where the summation is over all the *i* quantum states and ε_i are the discrete energy levels and δ is Dirac function.

1.5.2 Density of States for a One-Dimensional (ID) Structure

For ID structure like quantum wire, a particle (e.g., charge carrier) can move in one direction and in other two directions it is confined. The potential in two directions in infinitely large but in the third direction it is zero. The density of states in this case is expressed as

$$D(E) = \frac{dN}{dE} = \sum_{(1<E} (E - (i)½ \qquad \ldots(1.5)$$

Whereε_i are discrete energy levels. The graphical representation of density of states for 1D structure is shown in above figure A.

1.5.3 Density of States for Two-Dimensional (2D) Structures

For 2D structures which is basically a thin film structure (two directions long, one direction < 100 nm). The density of states is given by

$$\mathbf{D(}E\mathbf{) = 0 \text{ for } E < \varepsilon_I}$$

$$\mathbf{= 1 \text{ for } E > \varepsilon_I} \qquad \ldots(1.6)$$

Where ε_I is the *i*th energy level within 2D quantum well

The graphical representation of density of states for 2D structure, a staircase structure, is shown in Fig. A.

1.5.4. Density of States for Three-Dimensional (3D) Structures

For a 3D structure which is equivalent to a three-dimensional box of length *a*, width *b* and height *c* with potential $V = 0$ inside the box and $V = \infty$ outside the box, the solution of Schrodinger equation shows that the energy states are:

$$E_{n_x,n_y,n_z} = \frac{(h^2)}{8*m*a^2} (n^2_x + n^2_y + n^2_z)$$

And the density of states in this case

$$D\,(E) \propto E^{½} \qquad \ldots(1.7)$$

And the variation of density of states with respect to energy is shown in the figure.

Chapter 2

Nanostructure Semiconductors: Physics and Applications

2.1. Introduction

Nanometer range semiconducting materials have been a subject of intense study for last several years due to their size dependent physical and chemical properties below a critical size characteristic of the material. Blue-shift in the optical absorption spectrum, size dependent luminescence, enhanced oscillator strength; nonlinear optical effects are some examples of the interesting properties exhibited by these nanocrystals. All these properties are various manifestations of the so called size quantization effect which arises due to the increasing quantum diminishing size of the crystallites and the consequent changes in the electronic structures. Their electronic structure is between that of a molecule and a bulk responsible to give rise to profound modification of the physical properties. Nanoparticles have been suggested for various potential applications in electronics where quantum confinement effects may be advantage. For examples, quantum confinement effects in nanostructured semiconductors results in widening the band gap of semiconductor and act as an efficient light emitter.

Also these Nanoparticles can be used to produce light of various colors by band gap tuning using particle size effects. As the life times of electrons in the excited states are large, therefore they can be used in laser application. It has also got technological importance in the field of solar cells catalysis, light emitting, resonant tunneling devices, lasers, gas sensors and ultra violet sensors etc.

2.1.1. Cadmium Selenide Nanoparticles

Cadmium selenide is an inorganic compound with the formula CdSe. It is a yellow-orange solid that is classified as an II-VI semiconductor of the n-type. There are three crystalline forms of CdSe known as wurtzite (hexagonal), sphalerite (cubic) and rock-salt (cubic). The sphalerite CdSe structure is unstable and converts to the wurtzite form upon moderate heating. The transition starts at about 130 °C, and at 700 °C it completes within a day. The rock-salt structure is only observed under high pressure.

CdSe-derived nanoparticles exhibit with sizes below 100 nm exhibit a property known as quantum confinement. Quantum confinement results when the electrons in a material are confined to a very small volume. By virtue of their size dependent fluorescence spectrum, CdSe is of interest in optical devices such as laser diodes, photo voltaic cell etc. Similarly CdSe-based materials have potential

uses in biomedical imaging. Human tissue is permeable to far infra-red light. By injecting appropriately prepared CdSe nanoparticles into injured tissue, it may be possible to image the tissue in those injured areas.

CdSe material is transparent to infra-red (IR) light and has seen limited use in windows for instruments utilizing IR light. The material is also highly luminescent.[2]

2.2 Synthesis of Nanostructure Semiconductors

There is substantial variation in electrical and optical properties when the crystalline size is comparable to Bohr exciton radius. For most of these semiconductors, Bohr exciton radius is less than 10-15 nm excepting few narrow gap semiconductors. Further, presence of a small amount of impurity causes dramatic changes in different properties of semiconductors. Thus, it is of great challenge to synthesize particles of nanometer dimension with narrow size distribution and without any impurity. There are different ways to synthesize nanoparticles are chemical deposition, sol-gel, gas evaporation, electrostatic deposition, magnetron sputtering and electrochemical deposition etc. Chemical bath deposition technique is relatively less expensive and convenient to prepare large area semiconductor thin films at moderate temperature. Materials can easily be prepared in the colloidal form which can subsequently be precipitated to give dry and stable powders or can be deposited in thin film form onto different substrates. The growth process involves a controllable chemical reaction which proceeds at a low rate in an aqueous solution containing various reactants. The reaction rate in this technique is controlled by adjusting pH, solution temperature, and the relative concentrations of various reactants in the solution.

For the samples prepared by the chemical route, it is expected to have the size distribution which ultimately will influence the experimental results. For example, each spectrum obtained for optical absorption and photoluminescence is a summation of the spectrum of individual crystallite. So, the optical absorption and photoluminescence spectra observed for chemically prepared nano-crystallite samples do not show any sharp feature originating from individual crystallite but show wide terraces. Thus, it is most essential to restrict the size distribution in nanocrystalline samples. In order to arrest the agglomeration of the nanocrystallites, the crystallites are generally capped with polymers such as thiophenol, mercaptoethanol, ethylene glycol or with solvent as oleic acid etc. For example, the chemical synthesis of binary semiconductors can be carried out by missing two salts each having one component. However, before missing two salts to obtain the desired semiconductor, the organic capping agent is added to either of the salts that control the size of the nanoparticles.

2.3 Physical Properties

Physical properties such as structure, phase, thickness, composition, surface roughness, crystalline shape and size are known to influence the nanocrystalline semiconductor properties. The observation of quantum confinement effect, interfacial as well as device properties basically depend upon above parameters.

2.3.1 Impurity Identification and Composition

As there are small number of atoms present in a cluster or nanostructure, the presence of impurity of foreign element or off-stoichiometry leads to structural defects causing dramatic changes in electrical and optical properties. For example impurities and off-stoichiometry in nanostructure semiconductors generate localized electronic energy levels within the forbidden gap. Due to quantum confinement effect these states are also quantized and form a continuum of localized states near the band edges and ultimately influence the optical properties. The localized states also participate in conduction mechanism of carriers and influence the electrical properties. Most commonly used tool to identify and estimate the impurity or composition are : particle induced X-ray emission (PIXE), energy dispersive analysis of X-rays (EDAX), Rutherford back scattering spectrometry (RBS), secondary ion mass spectrometry (SIMS), Auger electron spectroscopy (AES) and X-ray photoelectron spectroscopy (XPS).

2.3.2. Surface Roughness and Fractals

From the perspectives of application, surface roughness plays a major role in determining optical scattering and absorption, electrical resistivity, thickness and photoluminescence properties. The interfacial properties are also influenced by the surface structure which often show deviation from ideal behavior.[5] Surface roughness is particular has pronounced effect in Raman scattering experiments which normally is expected to show size dependent feature. The surface phonon mode intensity is likely to increase with increasing surface roughness.

Hence, in the competing mechanism, one would expect for the Raman yield, is in between the surface roughness contribution and the contribution due to the excitation energy. It is known that the roughness depend upon the thickness of the film. As the thickness of a film increases the roughness increases irrespective of the sample preparation procedure. Further, the measurement with different scanning length indicates that with increasing scanning length, the roughness increases and exhibits scaling behavior over large variation of length scales.

2.3.3. Structure, Size and Shape of Nanocrystals

The structure and phase of the nano-crystals are in general determined by X-Ray Diffraction (XRD) and transmission electron microscopic studies. The structure of the nanocrystals depends on the sample preparation procedure, lattice strain and pressure. For example, chemically prepared CdSe at high temperature (350K) give a hexagonal phase whereas that prepared at 270K show a cubic phase, Further, the XRD peak intensity and width decreases with decreasing crystalline size. The peaks may shift to the high diffraction angle if there is lattice contraction caused by narrowing the crystalline size. Generally, the information regarding crystalline shape and size can be estimated from electron micrographs (TEM) or AFM images whereas the structural information can be obtained from XRD or from TEM diffraction studies. The shape of the crystalline is decided by the internal bonding geometry. Thus, for covalent crystals, such as Si and InP tetrahedral shape characteristic of the zinc blend and diamond interior bonding is favored. For ionic semiconductors *viz*. CdS or CdSe, hexagonal shape is favoured.[3] Hence, CdS crystallites prepared by a chemical route show exclusively a hexagonal phase contrary to the bulk zinc blende/wurzite structure. Nano-crystalline semiconductor shape and size can also be identified by optical absorption studies. Also with increasing crystalline size, the full width at half maximum (FWHM) decreases and the XRD peaks go sharper.

Chapter 3

Quantum Dots

3.1. Introduction

Materials science and technology is a field that is evolving at very fast pace and is currently giving the most significant contributions to nanoscale research. It is driven by the desire to fabricate materials with novel or improved properties. Such properties can be, for instance, strength, electrical and thermal conductivity, optical response, elasticity, or wear resistance. In electronics, the design and the assembly of functional materials and devices based on nanoscale building blocks can be seen as the natural, inevitable evolution of the trend toward miniaturization. The microelectronics industry, for instance, is fabricating integrated circuits and storage media whose basic units are approaching the size of few tens of nanometers. For computers, "smaller" means higher computational power at lower cost and with higher portability. However, this race toward higher performance is driving current silicon-based electronics to the limits of its capability. [3-6]

Fortunately, the advent of new methods for the controlled production of nanoscale materials has provided new tools that can be adapted for this purpose. New terms such as nanotubes, nanowires, and quantums dots are now common jargon of scientific publications. These objects are among the smallest man-made units that display physical and chemical properties which make them promising candidates as fundamental building blocks for novel transistors. The advantages envisaged here are higher device versatility, faster switching speed, lower power dissipation, and the possibility of packing many more transistors on a single chip.

With a completely different objective, the pharmaceutical and biomedical industries try to synthesize large supramolecular assemblies and artificial devices that mimic the complex mechanisms of nature or that can be potentially used for more efficient diagnoses and better cures for diseases. Examples in this direction are nanocapsules such as liposome's, embodying drugs that can be selectively released in living organs, or bioconjugate assemblies of biomolecules and magnetic (or fluorescent) nanoparticles that may provide faster and more selective analysis of biotissues. These prototype systems may one day evolve into more complex nanomachines with highly sophisticated functional features able to carry out complicated tasks at the cellular level in a living body.

Quantum dots are semiconductors composed of atoms from groups II – VI or III – V elements of the periodic table, for example, CdSe, CdTe, and InP[10]. Their brightness is attributed to the quantization of

energy levels due to confinement of an electron in a three-dimensional box. The optical properties of quantum dots can be manipulated by synthesizing a (usually stabilizing) shell. Such Q-dots are known as core-shell quantum dots, for example, CdSe – ZnS, InP – ZnS, and InP – CdSe.

3.2. Nanoscale Materials and Quantum Mechanics

3.2.1. Nanoscale Materials as Intermediate between Atomic and Bulk Matter

Nanoscale materials frequently show behavior which is intermediate between that of a macroscopic solid and that of an atomic or molecular system. Consider, for instance, the case of an inorganic crystal composed of few atoms. Its properties will be different from those of a single atom, but we cannot imagine that they will be same as those of a bulk solid.

The number of atoms on the crystal's surface, for instance, is a significant fraction of the total number of atoms, and therefore will have a large influence on the overall properties of the crystal. We can easily imagine that this crystal might have a higher chemical reactivity that the corresponding bulk solid and that it will probably melt at lower temperatures. Consider now the example of a carbon nanotubes, which can be thought of as a sheet of graphite wrapped in such a way that the carbon atoms on one edge of the sheet are covalently bound to the atoms on the opposite edge of the sheet are covalently bound to the atoms on the opposite edge of the sheet. Unlike its individual components, a carbon nanotube is chemically extremely stable because the valences of all its carbon atoms are saturated. Moreover, we would guess that carbon nanotubes can be good conductors because electrons can freely move along these tiny, wire-like structures. Once again, we see that such nanoscopic objects can have properties which do not belong to the realm of their larger (bulk) or smaller (atoms) counterparts. These properties can only be explained by the laws of quantum mechanics.

3.2.2. Quantum Mechanics

A fundamental aspect of quantum mechanics is the particle-wave duality, introduced by De Broglie, according to which any particle can be associated with a matter wave whose wavelength is inversely proportional to the particle's linear momentum. Whenever the size of a physical system becomes comparable to the wavelength of the particles that interact with such a system, the behavior of the particles is best described by the rules of quantum mechanics (7). All the information we need about the particle is obtained by solving its Schrodinger equation. The solutions of this equation represent the possible physical states in which the system can be found. Fortunately, quantum mechanics is not required to describe the movement of objects in the macroscopic world. The wavelength associated with a macroscopic object is in fact much smaller than the object's size, and therefore the trajectory of such an

object can be excellently derived using the principles of classical mechanics. Things change, for instance, in the case of electrons orbiting around a nucleus, since their associated wavelength is of the same order of magnitude as the electron nucleus distance.

Whenever the size of a semiconductor solid becomes comparable to this wavelength, a free carrier confined in this structure will behave as a particle in a potential box [8]. The solutions of the Schrodinger equation in such case are standing waves confined in the potential well, and the energies associated with two distinct wave functions are, in general, different and discontinuous. This means that the particle energies cannot take on any arbitrary value, and the system exhibits a discrete energy level spectrum. Transitions between any two levels are seen as discrete peaks in the optical spectra, for instance. The system is then also referred to as "quantum confined". If all the dimensions of a semiconductor crystal shrink down to a few nanometers, the resulting system is called a "quantum dot" and will be the subject of our discussion throughout this chapter. The main point here is that in order to rationalize (or predict) the physical properties of nanoscale materials, such as their electrical and thermal conductivity or their absorption and emission spectra, we need first to determine their energy level structure.

3.3. From Atoms to Molecules and Quantum Dots

From the point of view of a chemist, the basic building blocks of matter are atomic nuclei and electrons. In an atom, electrons orbit around the single nucleus, and the number of Electrons depends on the element. In the orbits simplest case of hydrogen atom, one electron orbits around one proton. The electronic states of the hydrogen atom can be calculated analytically [9,10]. As soon as more than one electron is involved, however, the calculation of the energy levels becomes more complicated, since, in addition to the interaction between the nucleus and the electron, now also electron-electron interactions have to be taken into account. Although the energy states of many-electron interactions have to be taken into account. Although the energy states of many-electron atoms can no longer be derived analytically, approximations such as the Hartree-Fock method exist [10]. Each electron can be ascribed to an individual orbit, called an atomic orbital (AO), with an associated discrete energy level. Depending on the angular moment of the orbit, AOs can be spherical (*s-orbital*), or a more complicated (*d*-, *f*-orbitals) shape. The eight valence electrons of a neon atom, for example, occupy one *s*- and three *p*-orbitals around the nucleus, one spin up and one spin down per orbit [10], where the energy level of the s-orbital is lower than that of the *p*-orbitals. In accordance with the rules of quantum mechanics, the energy levels are discrete.The next bigger structure, obtained from the combination of several atoms, is the molecule. Now electrons orbit collectively around more than one nucleus. In a molecule, electrons that are responsible for the covalent bonds between individual atoms can no longer be ascribed to one individual atom, but they are "shared". In methane (CH_4), for instance, each of the four sp^3 atomic orbitals of the central carbon

atom is linearly combined with the *s* orbital of a hydrogen atom to form a bonding (σ)and an anti-bonding (σ*) orbital, respectively [9]. Since these orbitals are "shared" between the atoms, they are called molecular orbitals. Only the lowest energy (bonding) orbitals are occupied, and this explains the relative stability of methane [10]. Using the same principle, it is possible to derive the electronic structure of more complex systems such as large molecules or atomic clusters. When combining atoms to form a molecule, we start from discrete energy levels of the atomic orbitals and we still end up obtaining discrete levels for the molecular orbitals [9].

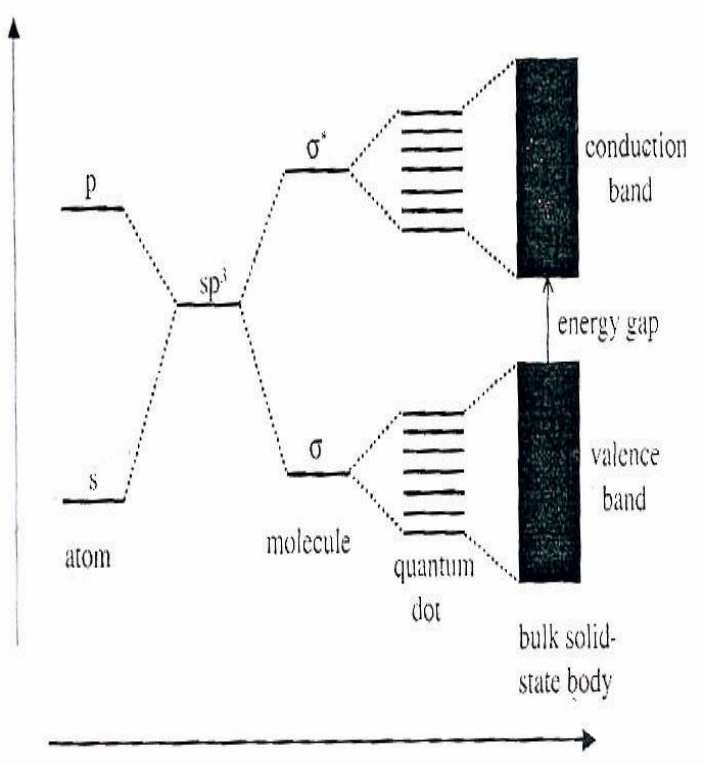

Figure B: Electronic energy levels depending on the number of bound atoms.

3.4. Energy Levels of a (Semiconductor) Quantum Dot

Some basic properties of semiconducting materials can be described by the model of free electrons and free holes. The energy bands for electrons and holes are separated by a band gap [14, 15]. The dispersion relations for the energy of electrons and holes in a semiconductor are parabolic at first approximation. This approximation holds true only for electrons (holes) occupying the levels that lie at the bottom (top) of the conduction (valence) band. Each parabola represents a quasi-continuous set of electron (hole) states along a given direction in k-space. The lowest unoccupied energy band and the highest occupied energy band are separated by an energy gap *Eg* (bulk), as shown in Figure. The band gap for a bulk semiconductor can range from a fraction of an *eV* up to a few *eV*.

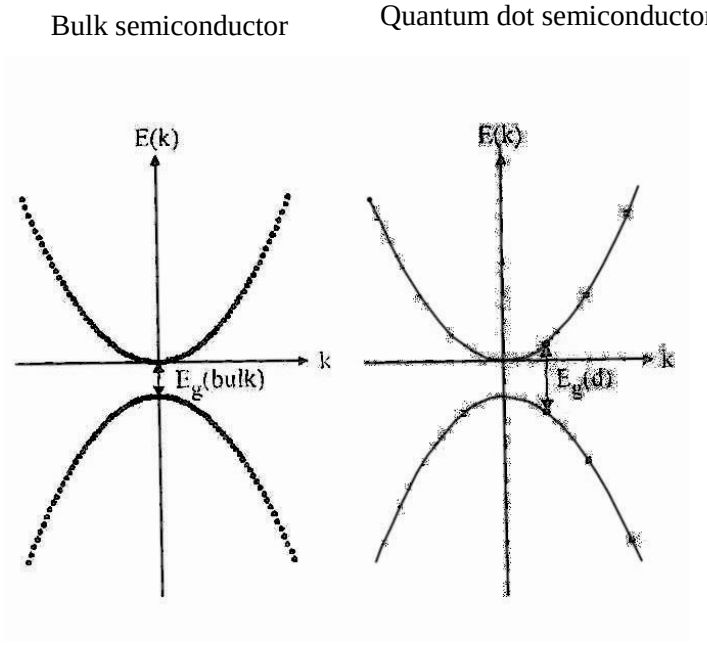

Fig. C: Dispersion relation for bulk and Quantum dot semiconductor

We might expect that the energy dispersion relations are still parabolic in a quantum dot. However, since only discrete energy levels can exist in a dot, each of the original parabolic bands of the bulk case is now fragmented into an ensemble of points. The energy levels of a quantum dot can be estimated with the particle-in-a-box mode. As described earlier , the lowest energy for an electron in a one-dimensional potential well as

$$\boldsymbol{E_{\text{well, 1d}}} = \frac{\boldsymbol{h^2}}{\boldsymbol{8 * m * a^2}} \qquad (3.1)$$

Here, *d* is the width of the well. In a quantum dot, the charge carriers are confined in all three dimensions, and this system can be described as an infinite 3-dimensional potential well. The potential energy is zero everywhere inside the well but is infinite on its walls. We can also call this well a "box". The simplest shapes of a three-dimensional box can be, for instance, a sphere or a cube. If the shape is cubic, the Schrodinger equation can be solved independently for each of the three translational degrees of freedom, and the overall zero-point energy is simply the sum of the individual zero point energies for each degree of freedom [9, 30]:

$$\boldsymbol{E_{\text{well, 3d (cube)}} = 3\, E_{\text{well, 1d}} = \frac{3*h^2}{8*m*a^2}} \qquad (3.2)$$

If the box is a sphere of diameter *d*, the Schrodinger equation can be solved by introducing spherical coordinates and by separating the equation into a radial part and a part that contains the angular momentum [31, 32]. The lowest energy level (with angular momentum = 0) is then

$$\boldsymbol{E_{well,\ 3d(sphere)} = \frac{h^2}{2*m*d^2}} \qquad (3.3)$$

The effect of quantum confinement is again remarkable. More confined charge carriers lead to a larger separation between the individual energy levels, as well as to a greater zero-point energy. If carriers are confined to a sphere of diameter *d*, the zero-point energy is higher than that for charge that are confined to a cube whose edge length is equal to d($E_{\text{well, 3d(sphere)}} > E_{\text{well, 3d(cube)}}$. This is because such sphere simply has a smaller volume ($\pi/6\ d^3$) than the cube (d^3).

An electron-hole pair can be generated in a quantum dot, for instance, by a photo induced process, or by charge injection. The minimum energy Eg required for creating an electron-hole pair in a quantum dot is made up of several contributions. One contribution is the bulk band gap energy, E_g(bulk). Another important contribution is the confinement energy for the carriers, which we call $E_{well} = E_{well}\ (E\text{-}) + E_{well}\ (h^+)$. For large particles (bulk: d $\rightarrow\infty$) E_{well} tends to zero. We can estimate the overall confinement energy for an electron-hole pair in a spherical quantum dot. It is the zero point energy of the potential well, or in other words, the energy of the state of a potential box with the lowest energy. This can be written as

$$\boldsymbol{E_{\text{well}} = \frac{h^2}{2*m^**d^2}} \qquad (3.4)$$

Where m* is the reduced mass of the exciton and is given by [33]

$$1/m^* = 1/m_e + 1/m_h \qquad (3.5)$$

Here m_e and m_h are the effective masses for electrons and holes, respectively. In order to calculate the energy required to create an electron-hole pair, another term (E_{Coul}) has to be considered. The Coulomb interaction E_{Coul} takes into account the mutual attraction between the electron and the hole, multiplied by a coefficient that describes the screening of the carriers by the crystal. In contrast to E_{well}, the physical meaning of this terms can be understood within the framework of classical electrodynamics. However, an estimate of such a term is only possible if the wave functions for the electron and the hole are known. The strength of the screening coefficient depends on the dielectric constant ε of the semiconductor. An estimate of the coulomb term yields.

$$\boldsymbol{E_{\mathbf{Coul}} = \frac{-1.8 * e^2}{2 * \pi * \varepsilon\varepsilon 0 * d}} \qquad (3.6)$$

This term can be quite significant, because the average distance between an electron and a hole in a quantum dot can be small [20, 34 – 37]. We can now estimate the size-dependent energy gap of a spherical semiconductor quantum dot, which is [33 – 37]:

$$\boldsymbol{E_g(\mathrm{dot}) = E_g(\mathrm{bulk}) + E_{well} + E_{Coul}} \qquad (3.7)$$

Then, by inserting above Eqs., we get:

$$\boldsymbol{E_g(\mathrm{d}) = E_g(\mathrm{bulk}) + \frac{h^2}{2 * m^* d^2} + \frac{-1.8 * e^2}{2 * \pi * \varepsilon\varepsilon 0 * d}} \qquad (3.8)$$

3.5. Colloidal Quantum Dots

Colloidal quantum dots are chemically synthesized using wet chemistry and are free standing nanoparticles or nanocrystals grown in solution [21].

In the fabrication of colloidal nanocrystals, the reaction chamber is a reactor containing a liquid mixture of compounds that controls the nucleation and the growth. The key parameter in the controlled growth of colloidal nanocrystals is the presence of one or more molecular species in the reactor which is generally termed as “surfactants”.

A surfactant is a molecule that is dynamically adsorbed to the surface of the growing quantum dot under the reaction conditions, which are mobile enough to provide access for the addition of monomer units and also stable enough to prevent the aggregation of nanocrystals.

The choice of surfactants varies from case to case, some examples of a suitable surfactant are alkyl thiols, phosphines, amides, carboxylic acids and nitrogen – containing aromatic.

As colloidal nanocrystals are dispersed in solution, they are not bound to any solid support, therefore they can be produced in large quantities in a reaction flask and can later be transferred to any desired substrate or object.

3.5.1. Optical properties of quantum dots: Absorption and Emission Spectra

The most striking effect in semiconductor nanoparticles is the widening of the gap Eg between the conduction band and valence band. This directly affects the optical properties of quantum dots as compared to the corresponding bulk material. Since the band gap depends on the size of a quantum dot, the onset of absorption is also size dependent.[20].

Excitons in semiconductors have a finite lifetime because of the recombination of the photo- excited electron – whole pair; therefore there is radiative decay through emission of photons or fluorescence. The wavelength of the fluorescence is longer than that of the absorbed light.

And the shift between the lowest energy peak in the absorption spectrum of a quantum dots and the corresponding emission peak is called the "stokes shift"[9].

The stokes shifts between absorption and emission maxima of quantum dots remain relatively constant. Because of additional nearby energy levels, quantum dots can be excited by photons of greater than or only slightly higher energies. Therefore, the effective Stokes shift can be hundreds of nanometers, permitting the excitation of numerous quantum dots possessing various emission maxima with the same excitation wavelength and this allows the simultaneous detection of numerous events.

3.5.2. Luminescence Lifetimes of Q-Dots

The photo physical properties of quantum dots are quite complicated as they are known to exhibit fluorescence intermittency, or blinking, over a wide range of time scales. Furthermore, variability within Q-dots samples leads to nonuniform fluorescence lifetimes. Concerning their excited-state lifetimes, quantum dots differ from traditional organic chromophores.

The position of the luminescence peak is also dependent on the average quantum dot size, and its width is correlated to the nanocrystals size distribution. Consequently, the maximum of the emission spectrum and its width can be used to estimate the mean size and the size distribution during nanocrystal growth.'

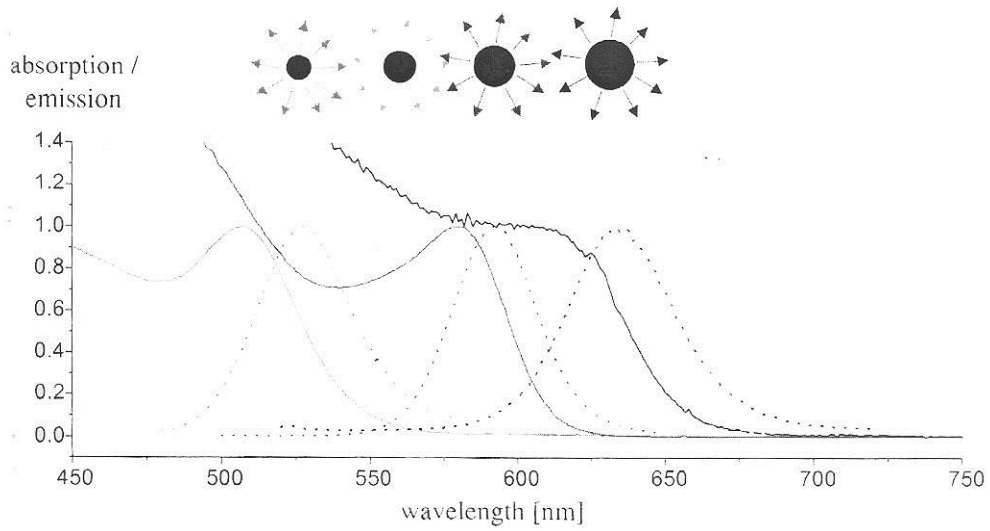

Fig. D: Absorption and emission spectra of colloidal CdSe Quantum dots of different sizes.

Chapter-4

Synthesis and Characterizations

4.1. Historical Review

4.1.1. Synthesis and Characterization of II-VI Nanoparticles

The field of "synthesis" or "preparation" of II-VI semiconductor nanoparticles has experienced and enormous development in the past two decades. The literature dealing with this topic is virtually unmanageable.

Even the shortest history of the preparation of II-VI semiconductor nanoparticles has started with the work published by A.Henglein in 1982 [1]. Like other [2-7], this paper deals with surface chemistry, photo degradation, and catalytic processes in colloidal semiconductor particles. But it is very work which reveals the first absorption spectrum of a colloidal solution of size-quantized CdSnanocrystals. These were prepared from $Cd(ClO_4)_2$ and Na_2S on the surface of commercial silica particles from the given figure we can see that, absorption onset is shifted considerably to the higher energies with respect to the bulk band gap of CdS (515nm). In addition, the sol emits light upon excitation at 390 nm, which is also a matter of investigation in this paper. The first correct interpretation of the observed blue shift of the absorption as a quantum mechanical effect is due to L Brus [8]. In the framework of the effective mass approximation, the shift in the kinetic energy of the charge carriers due to their spatial restriction to the volume of the nanometer-sized semiconductors is calculated.

Another milestone in the preparation of II-VI semiconductor nanocrystals is the work by Murray, Norris and Bawendi from 1993 [11]. Their synthesis is based on the pyrolysis of organometallic reagents like dimethyl cadmium and trioctylphosphine selenide after injection into a hot coordinating solvent. This approach provides temporally discrete nucleation and permits a controlled growth of the nanocrystals. Figure 4.1 shows the evolution of the absorption spectra of a series of CdSe crystallites ranging in size from about 1.2 to 11.5 nm. This series spans a range of sizes from more or less molecular species to fragments of the bulk lattice containing

Tens of thousands of atoms. The remarkable quality of these particles is clearly seen in several features of the absorption spectra, e.g., the steepness of the absorption onset, the narrow absorption bands, and the occurrence of higher energy transitions.

Yet another theoretical paper [20], it was again L. Brus who published in 1986 a review-like article [21] summarizing the then current status in the field of semiconductor clusters, from both an experimental and a theoretical view point. Also in 1986, attempts at a fractional separation by exclusion chromatography of an as-prepared sol of hexametaphosphate (HMP)- stabilized CdS particles were presented, together with stopped-flow experiments on extremely small clusters [22]. The binding of simple amines to the surface of CdS particles of various sizes prepared by conventional routes as well as in AOT/H_2O/heptanes reverse micelles enhances their luminescence quantum yield dramatically [23]. New preparative

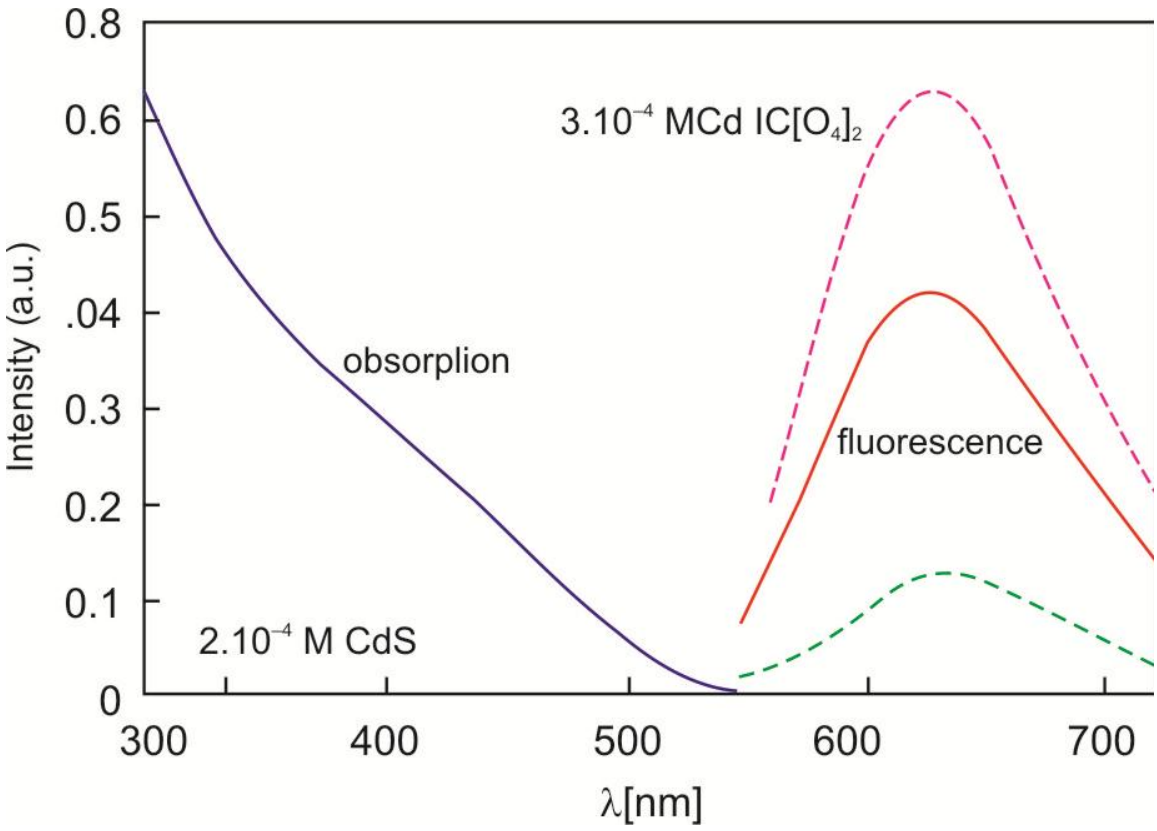

Figure E: Absorption and emission spectra of a colloidal CdS solution.

approaches were presented, e.g., the preparation of CdS particles in dihexadecyl phosphate (DHP) surfactant vesicles [24] and the synthesis of colloidal CdSe [25], which has now become the most important model system for the investigation of the properties of nanocrystalline matter.

4.1.2. Thiol-Stablized Nanoparticles

The use of thiols as capping agents in the synthesis of II-VI semiconductor nano-crystals has been very important part of the preparation techniques e.g. the dissolution of a metal salt in water in the presence of a stabilizing thiol, yields nanocrystals of CdSe, CdTe, HgTe, and CdHgTe. The thiols used in this work were 1-thioglycerol, 2-mercaptoethanol, 1-mercapto-2-propanol and cysteamine. Subsequent to the first steps in the preparation, heating of the reaction solution may be applied in order to initiate particle growth. Thus, this preparative approach relies on the separation of nucleation and growth in a way very similar to the organometallic TOP/TOPO preparation.

4.1.3. The "TOP/TOPO" Synthesis

The term "TOP/TOPO" synthesis refers to an organometallic approach to synthesizing CdSe nanocrystals was first introduced in 1993 by Murray et al.[11]. The preparative route is based on the pyrolysis of organometallic reagents (like dimethylcadmium) by injection into hot coordination solvents (like TOP/TOPO). This provides temporally discrete nucleation and permits the controlled growth of nanocrystals. Subsequent size-selective precipitation isolates samples with very narrow size distributions. The widespread success of this preparation is largely due to its versatility, its reproducibility and, last but not least, the high quality of the particles in terms of crystallinity and uniformity. The years immediately after the "invention" of the TOP/TOPO preparation are characterized by investigations into the optical properties of CdSe particles of a wide range of sizes and the surface properties of the evolving nanoparticles. Alternative routes high quality CdSenaocrystals are discovered by Qu, Peng and Peng by varying the solvents/ligands and the precursors like CdO and Cd (Ac)2 instead of Cd(CH3)2.

4.2. Green Chemistry Techniques

This is a technique we have used in the present work to synthesize CdSe nanoparticles as we have used green reagent such as paraffin liquid and the oleic acid as solvent. In the present work the green precursor CdO powder, Se powder has beenchoosen as the Cd source and Se source respectively.

Paraffin liquid is selected as the solvent (whose molecular formula can be expressed as CH_3 $(CH_2)_n$ CH_3, (n=16 – 22), which is colorless liquid at room temperature and boiled at above 300^0C.

As a solvent it is cheaper, environmentally friendlier and more stable in the atmosphere then the other solvents such as TOPO or ODE.

In the previous TOP-based route, it was acknowledged that role of the TOP or TBP solvents was to dissolve Se powder to form homogeneous Se solution. Whereas, in the present work, it is found that homogeneous Se solution is formed by simply heating Se powder with paraffin liquid during rapid stirring.

Also a natural product oleic acid is used as the acid which is much cheaper and environmentally friendlier than Hexylphosphonic Acid (HPA) or (TDPA).

4.2.1. Effect of Oleic Acid on the Growth of CdSe Nanocrystals

Oleic acid is not only acted as an efficacious capping agent for CdSe nanocrystals, but it markedly influences the primary nucleation steps in two distinct ways.

First, the number of nuclei is reduced drastically as oleic acid is added since the nucleation is more difficult in the presence of oleic acid due to its complexation with Cd.

Secondly complexing agent not only reduces the rate of nucleation by reducing the active monomer concentration, but it also rapidly caps the nuclei as they form.

These two effects compete with each other. If there is too much capping agent, nucleation can be completely hindered, ultimately leading to indiscriminate growth of a small population of nuclei. Thus we conclude that capping agents not only determine the rate of growth, but also play a major role in determining the number and size of the nuclei formed during injection; this, in turn, has a very pronounce influence on the subsequent growth rate.[38]

4.3. Characterization Techniques

The synthesized materials were characterized using X-Ray diffraction (XRD), Raman spectroscopy, Scanning electron microscope (SEM), Transmission electron microscope (TEM), Fourier transform Infra red Spectroscopy (FTIR) and TGA/DSC instruments. Structural and phase analysis are done by using XRD RigakuMiniflex-II diffractometer (Cu Kα = 1.54A^0), TEM was carried out using a JEM-2100F (GOEL electron microscope) 200k V and SEM was carried out by using (SEM, Hitachi S–3700). An FTIR spectrum was recorded with a single beam Perkin Elmer instrument (Spectrum BX-500) FT – IR Model spectrophotometer.

4.3.1. X-ray Diffraction

X-ray diffraction (XRD) is a versatile, non-destructive analytical technique for identification and quantitative determination of the various crystalline forms, known as "phase" of compounds present in powered and solid samples. The result of an XRD measurement is called a XRD pattern or diffractogram, showing phases present, phase concentrations, amorphous content and crystallite size; which are analyzed from peak positions, peak heights, background bump and peak widths respectively.

Identification is achieved by comparing the diffractogram obtained from an unknown sample with an internationally recognized database containing reference patterns called JCPDS.

Theory: A crystal lattice is a regular 3-dimensional distribution of atoms in space. These are arranged so that they form a series of parallel planes separated from one another by a distance d, which varies according to the nature of the material. For any crystal, planes exist in a number of different orientations, each with its own specific d-spacing.

When a monochromatic X-ray beam with wavelength λ is incident on lattice planes in a crystal at an angle θ, diffraction occurs only when the distance travelled by the rays reflected from successive planes differ by a complete number n of wavelength. By varying the angle θ, the Bragg's law ($n\lambda = 2d\sin\theta$) (Figure F) conditions are satisfied by different d-spacing in polycrystalline materials. Plotting the angular positions and intensities of the resultant diffraction peaks produces a pattern which is characteristic of the sample. Where a mixture of different phases is present, the diffractogram is formed by addition of the individual patterns.

Utility of XRD for Nanomaterials: Many structural properties of the nanostructures such as crystalline phase, particle size and structure evolution in Bragg planes, macroscopic stress/strain etc. can be revealed with the help of XRD. But here we shall mention few aspects directly relevant to our work.

Crystal Identification: A new method has been attempted-to-prepare nanomaterials. Therefore, it is important to identify these materials with the help of XRD data; we can check the amorphous or crystalline nature of the newly formed material. We can determine if the prepared material is crystalline and its basic lattice structure (e.g. cubic or hexagonal, etc.) by indexing its lattice plans. One can also determine the changes in various lattice parameters of a particular bulk and nanosized material.

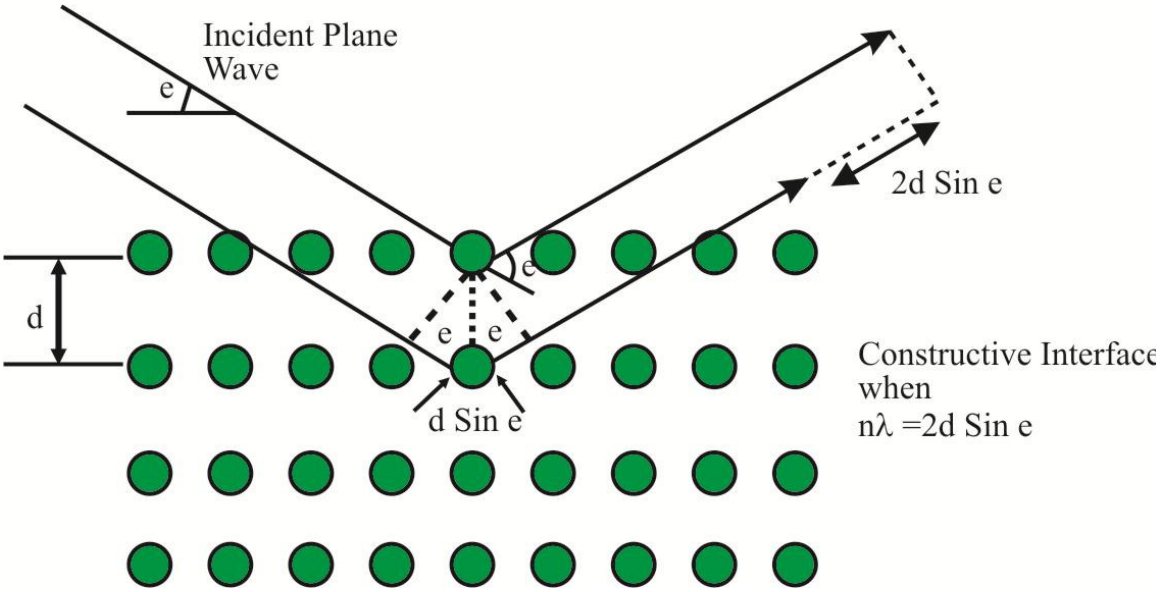

Figure F: diagram showing Bragg diffraction from a set of planes crystallite Size

Crystallite Size: A perfect crystal would extend in all directions to infinity, so we can say that no crystal is perfect due to its finite size. This deviation from perfect crystallinity leads to a broadening of the diffraction peaks. However, above a certain size (100-500nm) this type of broadening is negligible. Scherrer (1918) first observed that small crystallite size could give rise to line broadening. He derived a well-known equation for relating the crystallite size to the broadening, which is called Debye-Scherrer Formula is given by:

$$Dv = \frac{k\lambda}{\beta cos\theta} \quad \text{…. (4.1)}$$

Where, Dv = Volume weighted crystallite size. D is the "average" dimension of the crystallites normal to the reflecting planes. We call it "average" because the x-ray beam irradiates a large number of crystallites, so that the value of D obtained represents the mean value of the actual size distribution present, λ = wavelength of the radiation, k = Scherrer constant. K varies from 0.89 to 1, but for most cases, is close to 1, β = the integral breadth of a reflection (in radians 2θ) located at 2θ commonly considered as the full width at half maxima (FWHM) in radians for a certain peak position 2θ. Value of Scherer constant used at NPL is 0.89.

Crystallite size is a measure of the size of a coherently diffracting domain. Due to the presence of polycrystalline aggregates, crystallite size is not generally the same thing as particle size. When crystallites are less than approximately 100 nm in size, appreciable broadening in x-ray diffraction lines will occur. These regions may, in fact, correspond to the actual size of the particles. At other times, however, these regions form "domains" in a larger particle and may be a distinguishing and important feature. In either case, the observed line broadening can be used to estimate the average size. In the simplest case where the particles are stress-free, the size is estimated from a single diffraction peak. However, in cases where stress may be present, a more robust method involving several diffraction peaks is required.

4.3.2. Raman Spectroscopy

Raman spectroscopy is a spectroscopic technique based on inelastic scattering of monochromatic light, usually from a laser source. Inelastic scattering means that the frequency of photons in monochromatic light changes upon interaction with a sample. Photons of the laser light are absorbed by the sample and then reemitted. Frequency of the reemitted photons is shifted up or down in comparison with original monochromatic frequency, which is called the Raman Effect.

This shift provides information about vibrational, rotational and other low frequency transitions in molecules. Raman spectroscopy can be used to study solid, liquid and gaseous samples.

Origin of Raman Effect: The Raman effect is based on molecular deformations in electric field E determined by molecular polarizability α. The laser beam can be considered as an oscillating electromagnetic wave with electrical vector E. upon interaction with the sample it induces electric dipole moment P = αE which deforms molecules. Because of periodical deformation, molecules start vibrating with characteristic frequency ν_m.

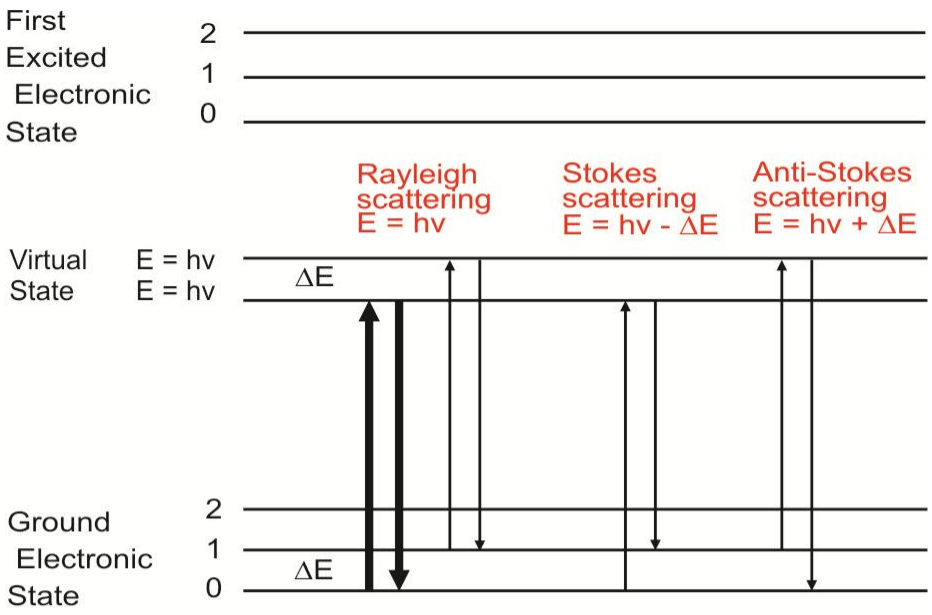

Different type of Scattering

Amplitude of vibration is called a nuclear displacement. In other words, monochromatic laser light with frequency v_o excites molecules and transforms them into oscillating dipoles. Such oscillating dipoles emit light of three different frequencies (FigureG)

1. A molecule with no Raman-active modes absorbs a photon with the frequency ν_0. The excited molecule returns back to the same basic vibrational state and emit light with the same frequency ν_0 as an excitation source. This type if interaction is called an elastic Rayleigh scattering.

2. A photon with frequency ν_0 is absorbed by Raman-active molecule which at the time of interaction is in the basic viberational state. Part of the photon's energy is transferred to the Raman-active mode with frequency ν_m and the resulting frequency of scattered light is reduced to $v_0 - v_m$. This Raman frequency is called Stokes frequency, or just "Stokes".

3. A photon with frequency ν_0 is absorbed by a Raman-active molecule, which, at the time of interaction, is already in the excited vibrational state. Excessive energy of excited Raman active mode is released, molecule return to the basic vibrational state and the resulting frequency of scattered light goes up to $\nu_0 + \nu_m$. This Raman frequency is called Anti-Stokes frequency, or just "Anti-Stokes".

4. About 99.999% of all incident photons in spontaneous Raman undergo elastic Rayleigh scattering. This type of signal is useless for practical purposes of molecular characterization. Only about 0.001% of the incident light produces inelastic Raman signal with frequencies $\nu_0 - \nu_m$. Spontaneous Raman scattering is very weak and special measures should be taken to distinguish it from the predominant Rayleigh scattering. Instruments such as notch filters, tunable filters, laser stop apertures, double and triple spectrometric systems are used to reduce Rayleigh scattering and obtain high quality Raman spectra.

Instrumentation

A Raman System typically consists of four major components:

1. Excitation source (Laser).
2. Sample illumination system and light collection optics.
3. Wavelength selector (Filter or Spectrophotometer).
4. Detector (Photodiode array, CCD or PMT).

A sample is normally illuminated with a laser beam in the ultraviolet (UV), visible (Vis) or near infrared (NIR) range. Scattered light is collected with a lens and is sent through interference filter or spectrophotometer to obtain Raman spectrum of a sample.

Since spontaneous Raman scattering is very weak the main difficulty of Raman spectroscopy is separating it from the intense Rayleigh scattering. More precisely, the major problem here is not the Rayleigh scattering itself, but the fact that the intensity of stray light from the Rayleigh scattering may greatly exceed the intensity of the useful Raman signal in the close proximity to the laser wavelength. In many cases the problem is resolved by simply cutting off the spectral range close to the laser line where the stray light has the most prominent effect. People use commercially available interference (notch) filters which cut-off spectral range of $\pm$ 80 – 120 cm^{-1} from the laser line. This method is efficient in stray light elimination but it does not allow detection of low-frequency Raman modes in the range below 100 cm^{-1}. Stray light is generated in the spectrometer mainly upon light dispersion on gratings and strongly depends on grating quality. Raman spectrometers typically use holographic gratings which normally have much less manufacturing defects in their structure then the rules once. Stray light produced by holographic gratings is about an order of magnitude less intense then from rules gratings of the same groove density. Using multiple dispersion stages is another way of stray light reduction. Double and triple spectrometers allow taking Raman spectra without use of notch filters. In such systems Raman-active modes with frequencies as low as 3-5 cm^{-1} can be efficiently detected. In earlier times people primarily used single-point detectors such as photon-counting Photomultiplier Tubes (PMT). However, a single Raman spectrum obtained with a PMT detector in wave number scanning mode was taking substantial period of time, slowing down any research or industrial activity based on Raman analytical technique. Nowadays, more and more often researchers use multi-channel detectors like Photodiode Arrays (PDA) or, more commonly, a Charge-Couple Devices (CCD) to detect the Raman scattered light. Sensitivity and

performance of modern CCD detectors are rapidly improving. In many cases CCD is becoming the detector of choice for Raman spectroscopy.

4.3.3. Scanning Electron Microscopy

Scanning electron microscopy (SEM) is a powerful and popular technique for imaging the surfaces of almost any material with a resolution down to about 1 nm. The scanning electron microscope (SEM) used a focused beam of high-energy electrons to generate a variety of signals at the surface of solid specimens. It utilizes the secondary electrons (SEs) and backscattered electrons (BSEs) being emitted from different areas of the specimen (as shown in Fig.H) as well as the trajectories they take in relation to the location of the detector. The signals that derive from electron sample interactions reveal information about the sample including its size, shape, external morphology (texture), of the three dimensional samples. The SEM is also capable of performing analyses of selected point locations on the sample, this approach is especially useful in qualitatively or semi-quantitatively determining chemical compositions (using EDS), crystalline structure, and crystal orientations (using EBSD). The design and function of the SEM is very similar to the EPMA, and considerable overlap in capabilities exists between the two instruments.

The image resolution offered by SEM depends not only on the property of the election probe, but also on the interaction of the electron probe with the specimen. Interactions of an incident electron beam with the specimen produce secondary electrons, with energies typically smaller than 50 eV, the emission efficiency of which sensitively depends on surface geometry, surface chemical characteristics and bulk chemical composition. The SEM has a large depth of field, which allows a large amount of the sample to be in focus at one time and produces an image that is a good representation of the three-dimensional sample.

The combination of higher magnification, larger depth of field, greater resolution, compositional and crystallographic information makes the SEM one of the most heavily used instruments in education institutions and laboratory research areas and industry.

The semiconducting nanoparticles were imaged using Hitachi S-3700 variable pressure SEM, of resolution 3nm with accelerating voltage of 0.3 to kV..

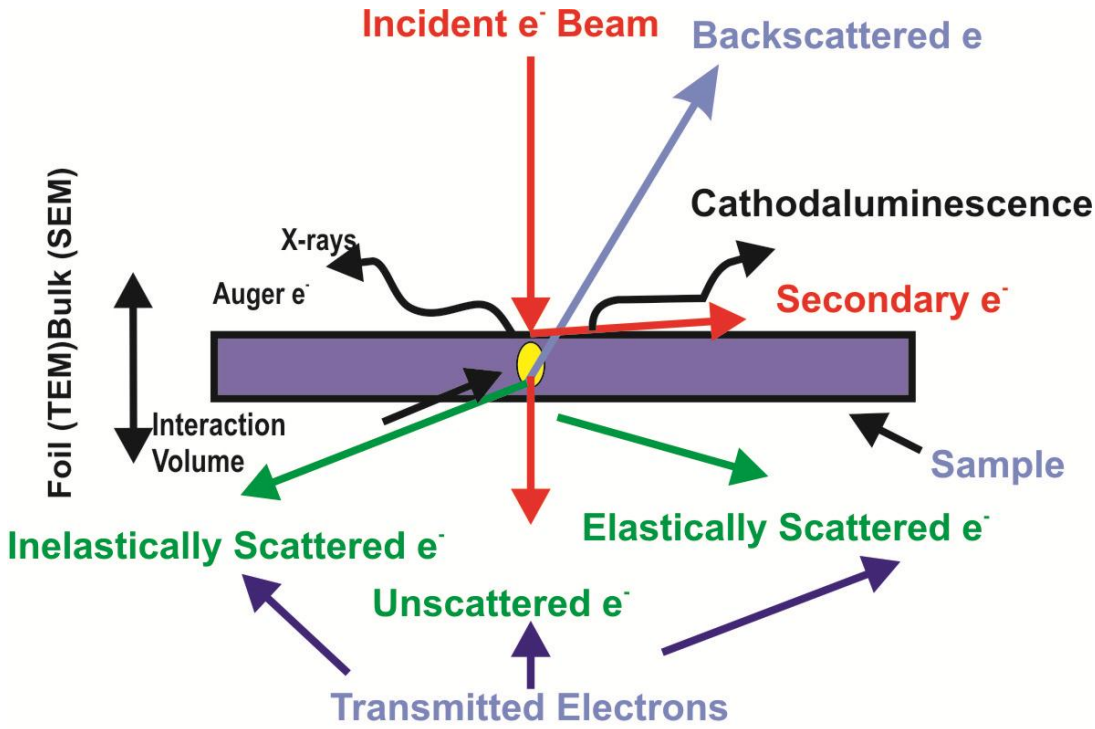

Interaction of high energy electrons with solid

Figure H:

4.3.4. Transmission electron microscopy

The Transmission electron microscopy (TEM) is a microscopy technique whereby a beam of electrons is transmitted through an ultra thin specimen, interacting with the specimen as it passes through. An image is formed from the interaction of the electrons transmitted through the specimen; the image is magnified and focused onto an imaging device, such as a fluorescent screen, on a layer of photographic film, or to be detected by a sensor such as a CCD camera. TEMs are capable of imaging at a significantly higher resolution that light microscopes, owing to the small de Broglie wavelength of electrons. This enables the instrument's use to examine fine detail – even as small as a single column of atoms, which is tens of thousands times smaller than the smallest resolvable object in a light microscope. TEM forms a major analysis method in a range of scientific fields, in both physical and biological sciences. At smaller magnifications TEM image contrast is due to absorption of electrons in the material, due to the thickness and composition of the material. At higher magnifications complex wave interactions modulate the intensity of the image, requiring expert analysis of observed image. Alternate modes of use allow for the TEM to observe modulations in chemical identity, crystal orientation, electronic structure and sample

induced electron phase shift as well as the regular absorption based imaging. The first TEM was built by Max Knoll and Ernst Ruska in 1931, with this group developing the first TEM with resolving power greater than that of light in 1933 and the first commercial TEM in 1939.

The TEM is composed of several components, which include a vacuum system in which the electrons travel an electron emission source for generation of the electron stream, a series of electromagnetic lenses, as well as electrostatic plates.

The latter two allow the operator to guide and manipulate the beam as required. Also required is a device to allow the insertion into, motion within, and removal of specimens from the beam path. Imaging devices are subsequently used to create an image from the electrons that exit the system.

Applications

The instrument allows performing the Morphological analysis, Electronic diffraction, X-EDS qualitative and semi-quantitative analysis, either in Spot or in Semi Stem mode. The instrumentation is particularly suitable for the study and characterization of material from a morphological, chemical and structural point of view, especially in the field of polymeric, metallic, and ceramic technology.

On the basis of available techniques, some specific applications in which the instrument plays an important role are:

- Nano-structured materials study
- Defects from the manufacturing process in semi-conductors
- Ceramic systems
- Plastic Deformations
- The study of layers and structures
- Phase transformations
- Nanometric systems
- Ordered alloy structures
- The study of cellular structures

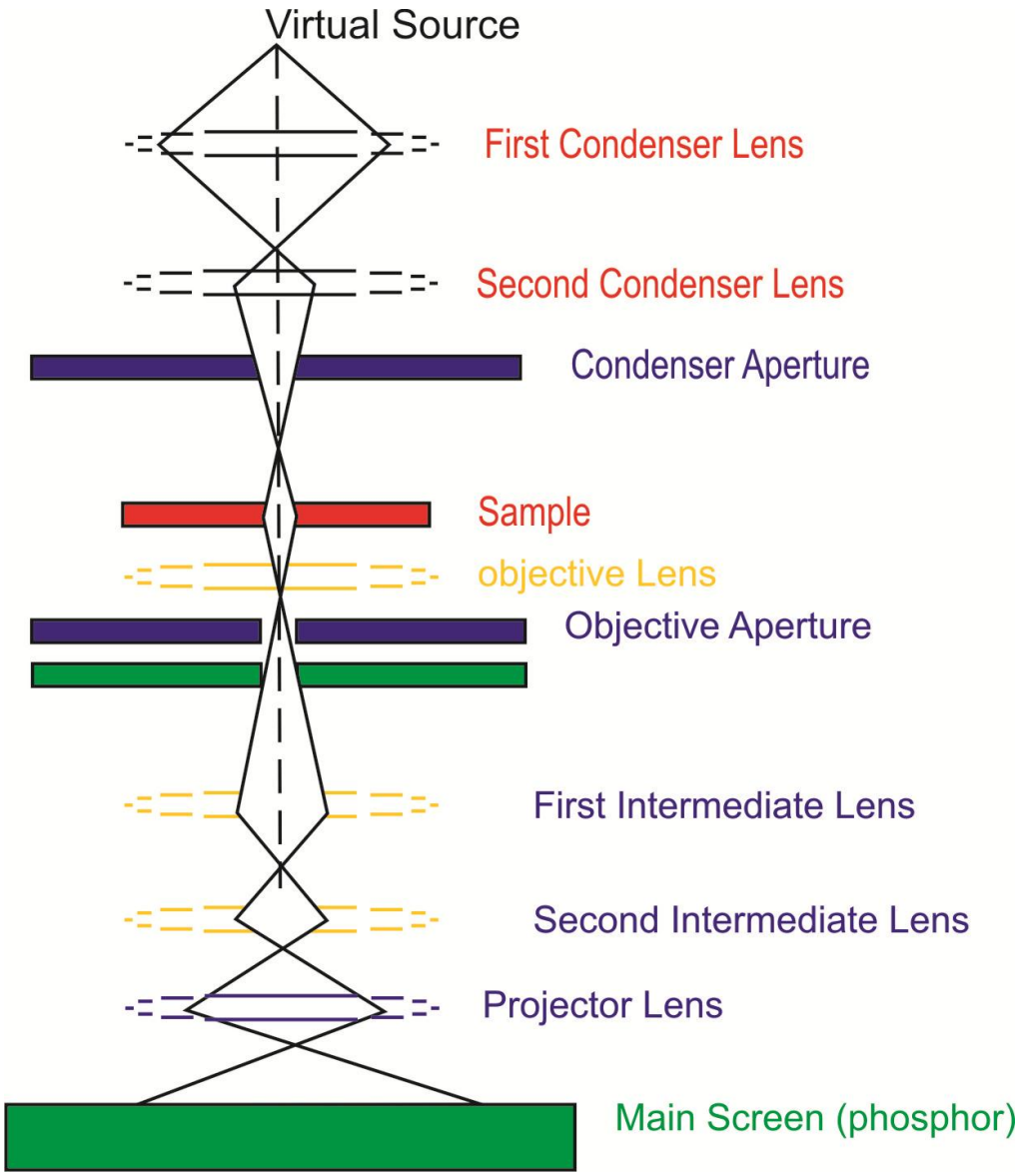

Fig. I : Transmission Electron Microscope.

Samples Used and Their Preparation

For viewing the morphology of the nanoparticles formed, nanoparticles were washed several times in methanol to remove the extra groups. Very dilute solutions of these washed nanoparticles in methanol were dropped on carbon coated meshed TEM grids and the solvent was allowed to evaporate leaving the nanoparticles on the grid. These grids were then loaded in the vacuum chamber of the microscope for viewing.

4.3.5 FTIR Spectroscopy

FTIR (Fourier Transform Infrared) or simply FTIR Analysis, is most useful technique for identifying chemicals that are either organic or inorganic. It can be utilized to quantities some components of an unknown mixture. It can be applied to the analysis of solids, liquids, and gasses. FTIR spectroscopy is a multiplexing technique, where all optical frequencies from the source are observed simultaneously over a period of time known as scan time. In this technique whole data is collected and converted from an interference pattern to a spectrum.

By interpreting the infrared absorption spectrum, the chemical bonds (functional groups) in a molecule or molecular structure of materials, whether organic or inorganic can be determined. FTIR spectra of pure compounds are generally so unique that they are like a molecular "fingerprint". While organic compounds have very rich, detailed spectra, inorganic compounds are usually much simpler. The technique works on the fact that bonds and groups of bonds vibrate at characteristic frequencies. A molecule that is exposed to infrared rays absorbs infrared energy at frequencies which are characteristic to that molecule i.e. those frequencies where the infrared light affects the dipolar moment of the molecule. Thus monatomic (He, Ne, Ar, etc) and homopolar diatomic (H2, N2, O2, etc) molecules do not absorb infrared light. During FTIR analysis, a spot on the specimen is subjected to a modulated IR beam. The specimen's transmittance and reflectance of the infrared rays at different frequencies is translated into an IR absorption plot consisting of reverse peaks. The resulting FTIR spectral pattern is then analyzed and matched with known signatures of identified materials in the FTIR library. RI absorption information is generally presented in the form of a spectrum with wavelength or wave number as the x-axis and absorption intensity or percent transmittance as the y-axis. Transmittance, T, is the ratio of radiant power transmitted by the sample (I) to the radiant on the sample (I_0). Absorbance (A) is the logarithm to the base 10 of the reciprocal of the transmittance (T).

$$A = \log_{10}\frac{\mathbf{1}}{T} = -\log 10\ T = -\log_{10}\frac{I}{I\mathbf{0}} \qquad \ldots \qquad (4.2)$$

The transmittance spectra provide better contrast between intensities of strong and weak bands because transmittance ranges from 0 to 100% T whereas absorbance ranges from infinity to zero.

In our case all FTIR spectra were recorded with a single beam Perkin Elmer instrument (Spectrum BX-500) FT-IR Model spectrophotometer Fig. 3.11. This spectrometer allows us to collect spectra in mid-IR far-IR and near-IR spectral ranges. The spectrum BX contains a CDRH Class II Helium Neon laser, which emits visible, continuous wave radiation at a wavelength of 633 nm and has a maximum output power of less than ImW.

The recording abscissa range of this instrument is 400-4000cm^{-1}. Each spectrum was collected with 64 scans co-added at 4cm^{-1} resolution. The normal operation mode of this spectrometer is temperature stabilized. The spectrometer utilizes continuous dynamic alignment to ensure exceptional high-resolution line shapes. Its compact optical path minimizes beam path length and improves spectral performance by limiting the number of beam reflections, which translates into extremely reproducible results with no instrument drift. Before measurement the instrument is properly sealed and desiccated. The desiccant protects the beam splitter and other optical components by reducing the amount of water vapor inside the spectrometer.

Chapter 5

Preparation and Characterizations of the Sample

5.1. Experimental

We have synthesized Cadmium Selenide nanoparticles by colloidal route method. The experimental set up, chemical used & synthesis process are described in following section.

5.1.1. Experimental Setup

In this method a rotamantle is employed for the heating purpose where the range of temperature is varied from 150^0 C to 270^0 C and heating rate is varied from 1^0C to 10^0C per minute. Also the speed of stirring can be adjusted according to the reactions. The three neck bottom flask is used as reaction vessel which can be easily put in rotamantle.

Inert reaction medium was required throughout the reaction so nitrogen gas was passed to the side mouth of the flask. Also thermometer was inserted through another side mouth of the flask throughout the reaction procedure to monitor the temperature.

5.1.2. Chemical Used

All chemicals used in these experiments are of good quality and used without any further purification.

i. **Cadmium Oxide (CdO)** – Purchase from Aldrich

ii. **Selenium Powder (Se)** – Purchase from Aldrich

iii. **Oleic Acid –** Technical grade

iv. **Paraffin Liquid** – Chemical grade

v. **Methanol –** (Analytical grade)

vi. **Toluene** – (Analytical grade)

Equipments

- Rotamantle
- 3 neck round bottom flask
- Stirrer hot plate
- Thermometer – range upto 300^0C
- Beaker – 50 ml.
- Syringe 10 ml.
- Vials

5.1.3. Synthesis

Synthesis of CdSe nanoparticles was carried out by taking CdO and Se precursor in the molar ratio 2:1.

And all the powder reagents were weighed with the help of analytical balance.

PROCEDURE

Sample 1.

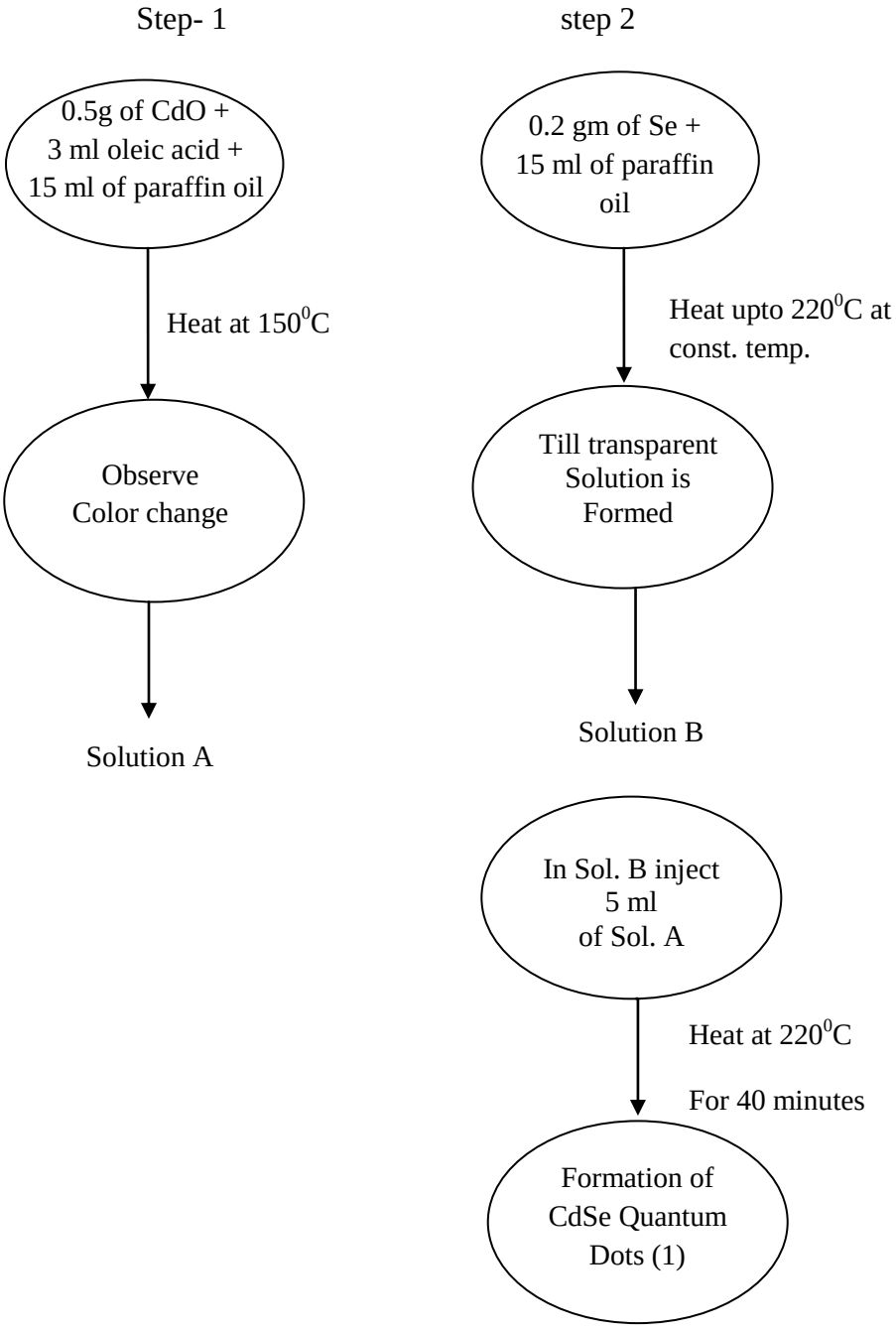

Figure J:

Cool the solution at room temperature and wash it with methanol several times and dried at 50^0C in vacuum oven.

5.2. Characterization

5.2.1. X-ray Diffraction Analysis

Structural and phase analysis of prepared sample has been carried out using X-ray diffractometer (XRD) with Cu-Kα (1.5418 A^0). The high intensity scan was recorded for 2θ range $10 – 80^0$.

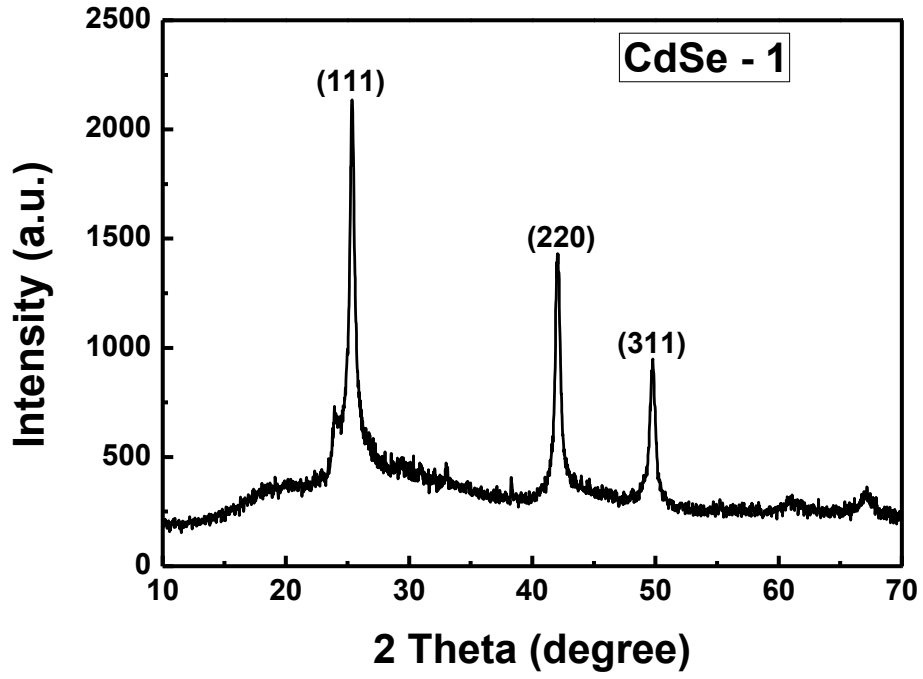

Figure -K

The powder X- ray diffraction patterns of synthesized sample is shown above.

The presence of peaks at 25.36^0 , 42.01^0 and at 49.72 ^{o} confirms the presence of cubic phase of CdSe nanoparticles according to JCPDS file .corresponding to planes as (111), (220) and (311) respectively.

The calculated Crystallite size of CdSe NCs comes out to be 1.63 nm. And the lattice constant was calculated by applying the formula :

$$a = d * (h^2 + k^2 + l^2)^{1/2} \qquad \text{where} \qquad d = \lambda/2 \sin \Theta$$

comes out to be 6.01 which was in good agreement of face centered lattice constant as 6.077.

5.2.2. Raman Spectroscopy

Raman spectra are used to analytically identify the phase formed. Spectra were recorded at room temperature with Ar^{+} laser beam of wavelength 514 nm incidents on the sample.

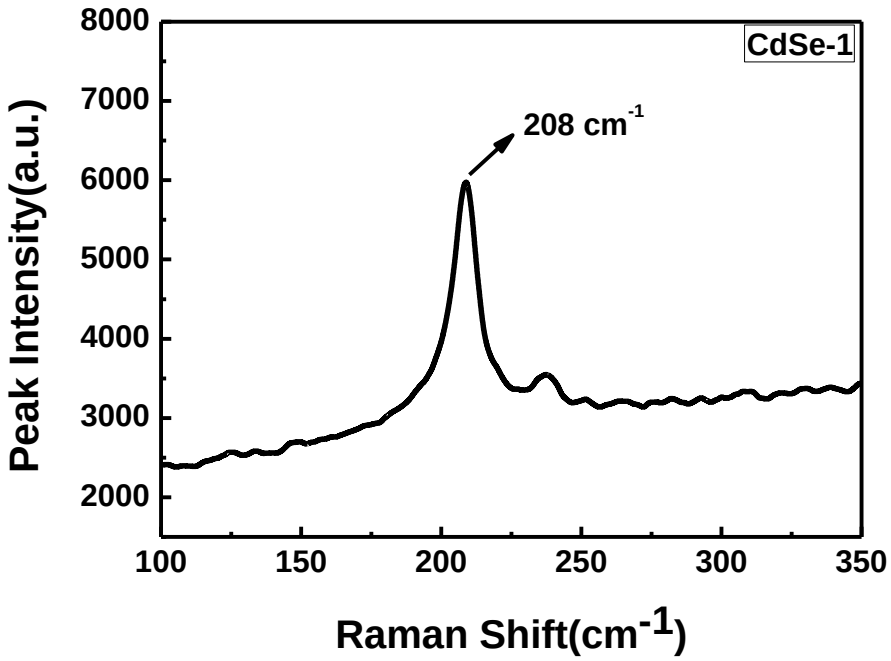

Figure -L

Since the Raman shift arises from the longitudinal optic phonon mode which is red shifted w.r.t bulk mode because of the phonon confinement, this can be seen from the data observed.

As we have observed Raman shift at 208 cm^{-1}

Where the bulk CdSe has $\nu_{(LO)}$ = 210 cm^{-1}

So we can conclude that XRD data was in good agreement with Raman data .

5.2.3. Scanning Electron Microscope

SEM images for analysis of morphology and structural shape of synthesized powder has been taken with Hitachi S-3700 SEM at 15 kV with appropriate magnification.

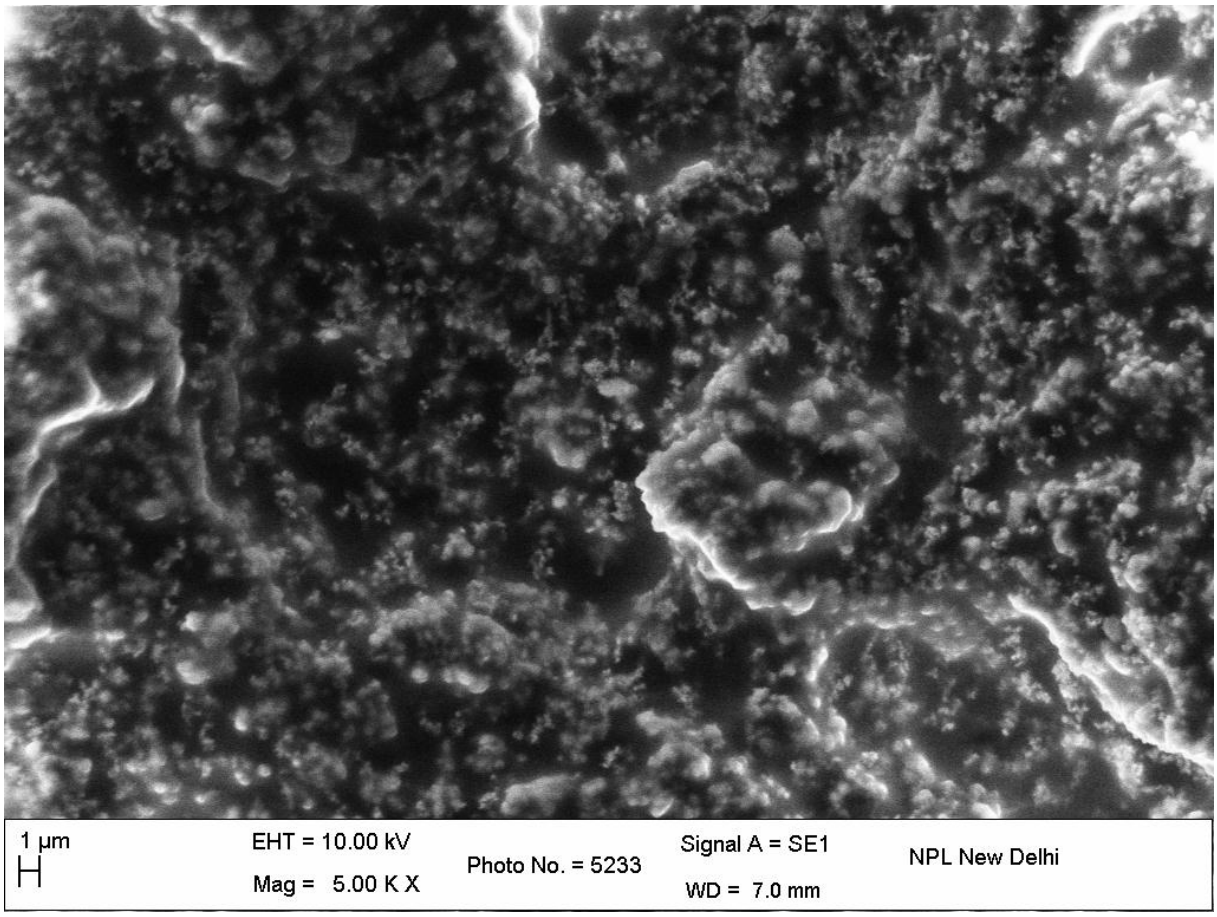

Figure: M

The observed surface morphology of CdSe nanoparticles shows that the particles are polycrystalline in nature.

5.2.4. Fourier Transform Infra-red Spectroscopy

FTIR spectroscopy is used to identify the attached functional group in a sample.

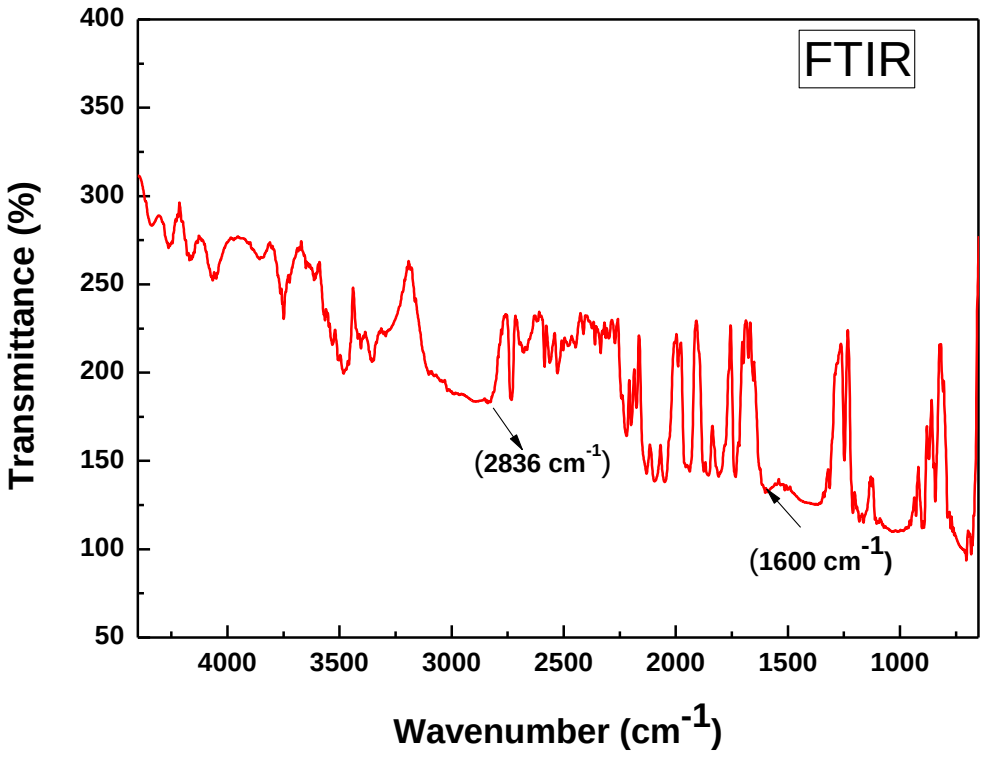

Figure -N

The FTIR spectrum shows the presence of capping ligand i.e Oleic acid on the surface of CdSe NCs at 1600 cm^{-1}. In general transmittance of Oleic acid lies in range of 1600 to 1750 cm^{-1}.

5.2.5 UV- Visible Spectrum :

The UV-Vis spectrum reveals the existence of two absorption , one at 430 nm and other at 665 nm.

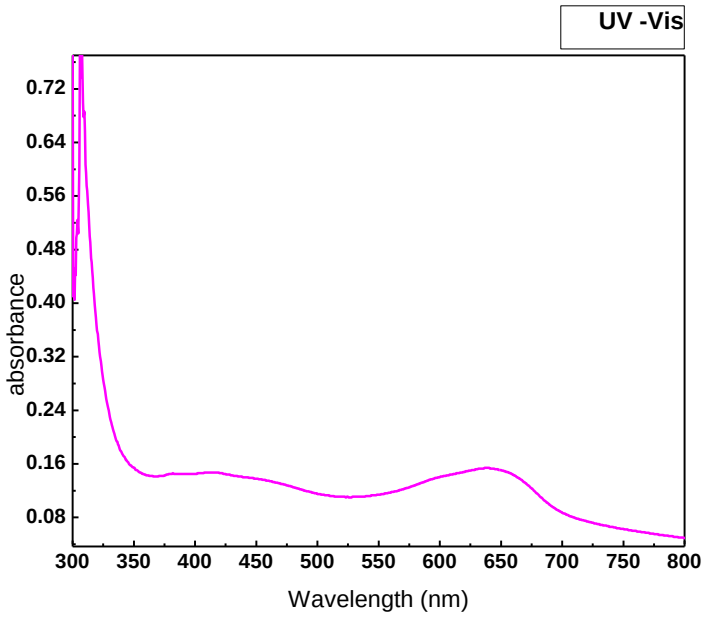

Figure O:

Absorption at 430 nm estimates the value of band gap energy in (eV) by taking tangent value of the curve as $\lambda = 525$nm gives Eg = 2.36 eV whereas absorption at 665nm results from the existence of surface state.

RESULTS AND DISCUSSION

In this thesis work we have successfully synthesized CdSe NCs. Low- cost and green reagents were used in the process. The role of the acid in the synthesis is to dissolve CdO powder and form homogeneous Cd solution and act as the capping ligand in the formation of the NCs. In the previous work (TOP- based route), it was acknowledged that the role of the TOP solvents was to dissolve Se powder to form homogeneous Se solution. However in the present study, it is found that homogeneous Se solution was formed by simply heating Se powder with paraffin liquid during rapid stirring. Also it is believed that the capping ligand Oleic acid not only determined the growth rate but also played a major role in determining the number and size of the nuclei formed during injection. [38]

X-Ray diffraction analysis:

The light brown color CdSe nanoparticles obtained after the completion of reaction and were characterized by various techniques to investigate their particle size and structural features. The XRD measurements of CdSe nanoparticles shows that the position of several diffracted peaks well with the standard powder diffraction data (FCC structure with a = 6.077). The several peaks (25.36^0, 42.01^0, and 49.72^0) of CdSe have been obtained due to diffraction form (111), (220) and (311) planes of Zinc blende (cubic) CdSe. And this result was also confirmed with the observed Raman shift in the Raman spectrum.

SEM analysis

The Scanning electron microscopy (SEM) image of the CdSe nanoparticles has been studied. The surface morphology of Cadmium Selenide shows that these materials are polycrystalline in nature.

UV-Visible analysis:

The electronic state is an important property and can be described in terms of valence and conductivity bands and a gap between these bands. However, as the particles become smaller, the wavelength of the electrons is closer to the range of the particle sizes and the laws of classical physics have to be substituted by Quantum confinement.

The UV-Vis spectrum showed the absorption at 430nm which is relatively blue shifted whereas the absorption at 665nm shows the existence of surface states which implies the incomplete capping of the CdSe surfaces.

CONCLUSION

In summary, we have developed a low- cost and green Non TOP- based route for synthesizing high quality Zinc – blended (cubic) CdSe NCs by using colloidal method. Choosing paraffin liquid and oleic acid as the reaction medium significantly simplified the reaction for green and low-cost. The average crystallite size of the resultant NCs comes out to be 1.36nm. The Raman shift also confirms the formation of CdSe nanoparticles. The FTIR study reveals the presence of capping ligand on the surface of nanoparticles. UV-Vis spectrum shows two humps at 430nm and at 665 nm. The absorbance at 665 nm results from the existence of surface states because of incomplete capped surface of CdSe NCs.

For future investigations we can work on these partially capped nanoparticles which may find applications in charge transfer devices. On the other hand, it is expected that the greater amount of surface capping agent would lead to a complete capping of the CdSe surface and the enhancement of the band –edge emission.

Reference

1. WILLEY-VCH Verlag GmbH & Co. KGaA, Weinheim ISBN : 3-527–30507–6
2. http://en.wikipedia.org/wiki/Cadmium_selenide
3. Kingon, A. I.; Maria, J.-P.; Streiffer, S. K. Nature 2000, 406, 1032–1038.
4. Lloyd, S. Nature 2000, 406, 1047–1054.
5. Ito, T.; Okazaki, S. Nature 2000, 406, 1027–1031.
6. Peercy, P. S. Nature 2000, 406, 1023–1026.
7. Cohen-Tannoudji, C.; Diu, B.; Laloe, F. Quantum Mechanics; 1st edn.; John Wiley & Sons: New York, 1997.
8. Yoffe, A. D. Adv. Physics 2001, 50, 1–208.
9. Atkins, P. W. Physical Chemistry; 3rd edn.; Oxford University Press: Oxford, 1986.
10. Karplus, M.; Porter, R. N. Atoms and Molecules; 1st edn.; W. A. Benjamin, Inc.: New York, 1970.
11. Harrison, W. A. Electronic Structure and the Properties of Solids: The Physics of the Chemical Bond; Dover Publications: Dover, 1989.
12. Burdett, J. K. Progress in Solid State Chemistry 1984, 15, 173–255.
13. Kittel, C. Einfu¨hrung in die Festko ¨rperphysik; 8th edn.; R. Oldenbourg Verlag: Mu¨nchen, Wien, 1989.
14. Ashcroft, N. W.; Mermin, N. D. Solid State Physics; Saunders College: Phiadelphia, 1976.
15. Van den Brom, H. E.; Yanson, A. I.; Ruitenbeek, J. M. Physica B 1998, 252, 69–75.
16. Bawendi, M. G.; Steigerwald, M. L.; Brus, L. E. Annu. Rev. Phys. Chem. 1990, 41, 477–496.
17. 51 Alivisatos, A. P. Science 1996, 271, 933–937.
18. Landau, L. D.; Lifschitz, E. M. Quantenmechanik; 9th edn.; Akademie-Verlag: Berlin, 1979; Vol. 3.
19. Schwabl, F. Quantenmechanik; 2nd edn.; Springer Verlag: Berlin, 1990.
20. Messiah, A. Quantenmechanik (Band 1); Walter de Gruyter: Berlin, 1976.
21. Trindade, T.; O'Brien, P.; Pickett, N. L. Chem. Mat. 2001, 13, 3843–3858.
22. Brus, L. E. J. Chem. Phys. 1983, 79, 5566–5571.
23. Brus, L. E. J. Chem. Phys. 1984, 80, 4403–4409.

24. Brus, L. J. Phys. Chem 1986, 90, 2555– 2560.

25. Steigerwald, M. L.; Brus, L. E. Acc. Chem. Res. 1990, 23, 183–188.

26. Fu¨hrer, A.; Lu¨scher, S.; Ihn, T.; Heinzel, T.; Ensslin, K.; Wegscheider, W.; Bichler, M. Nature 2001, 413, 822–825.

27. A. Henglein, Ber. Bunsenges. Phys. Chem. 1982, 86, 301.

28. K. Kalyanasundaram, E. Borgarello, D. Duonghong, M. Gra¨tzel, Angew. Chem., Int. Ed. Engl. 1981, 20, 987.

29. M. A. Fox, B. Lindig, C. C. Chem, J. Am. Chem. Soc. 1982, 104, 5828.

30. L. E. Brus, J. Chem. Phys. 1983, 79, 5566.

31. C. B. Murray, D. J. Norris, M. G. Bawendi, J. Am. Chem. Soc. 1993, 115, 8706.

32. L. E. Brus, J. Chem. Phys. 1984, 80, 4403.

33. L. E. Brus, J. Phys. Chem. 1986, 90, 2555.

34. C.-H. Fischer, H. Weller, A. Fojtik, C. Lume-Pereira, E. Janata, A. Henglein, Ber. Bunsenges. Phys. Chem. 1986, 90, 46.

35. T. Dannhauser, M. O'Neil, K. Johansson, D. Whitten, G. McLendon, J. Phys. Chem. 1986, 90, 6074.

36. Y.-M. Tricot, J. H. Fendler, J. Phys. Chem. 1986, 90, 3369.

37. J. M. Nemeljokvic, M. T. Nenadovic, O. I. Micic, A. J. Nozik, J. Phys. Chem. 1986, 90, 12.

38. Bullen C.R.;Mulvaney,P. Nano let. 2004, 4, 2303-2307